Available online at www.sciencedirect.com
ScienceDirect
Energy Reports 8 (2022) 880–886
www.elsevier.com/locate/egyr

2022 The 5th International Conference on Renewable Energy and Environment Engineering (REEE 2022), 24–26 August, 2022, Brest, France

# Control strategy for DC series-connected wind farm without energy curtailment

Jing Wu[a], Jian Qiu[a], Bo Dong[a], Ding Li[a], Lijun Xie[b,*], Xuesong Wang[a]

[a] China Electric Power Planning & Engineering Institute, Ande Road 65th, Xicheng District, Beijing, China
[b] China Electric Power Research Institute, Beijing, 100192, China

Received 7 October 2022; accepted 9 October 2022
Available online 29 October 2022

**Abstract**

With lower construction costs and power losses, the DC wind farm (DCWF) based on series-connected DC wind turbines (DCWT) is a potential collection scheme for large-scale offshore wind power. However, energy curtailment caused by unequal wind speed exists in DCWTs and results in energy waste, weakening the advantages of DCWTs. The energy curtailment mechanism is analyzed for DCWF, where single active bridge (SAB) is used as DC/DC converter in DCWTS and a full-bridge modular multilevel converter (FB-MMC) as the receiving end converter. The linear relationship between input and output of single active bridge (SAB) is interpreted, and a novel coordinate control strategy for DCWF is proposed to solve the wind energy curtailment caused by unequal wind speed. In addition, an auxiliary control strategy for receiving end converter is proposed to reduce the loss on HVDC link. A complete DCWF is built in PSCAD/EMTDC software package, and the results show that the proposed control strategy makes DCWF can operate well without energy curtailment under unequal wind speeds.


Peer-review under responsibility of the scientific committee of the 5th International Conference on Renewable Energy and Environment Engineering, REEE, 2022.

*Keywords:* DC wind farm; Control strategy; Single active bridge (SAB); Energy curtailment

## 1. Introduction

Offshore wind power is regarded as a promising energy with its environmentally friendly and nearly zero carbon. The high voltage direct current (HVDC)transmission technology is regarded as the best choice for long distance deep offshore wind farm integration [1–4]. However, an expensive offshore platform is needed to support the sending end station, which is difficult to build in the deep sea. To reduce investment and accelerate the development of offshore wind power transmission, a pure DCWF without offshore platform is proposed, where wind turbines are collected by DC lines [5,6].

Compared with parallel-connected or series-parallel-connected topologies, the series-connected topology is composed by several DCWTs with its DC output of DCWT series-connected in the DC collection system, and

* Corresponding author.
*E-mail address:* liju-xie@163.com (L. Xie).

https://doi.org/10.1016/j.egyr.2022.10.176


Peer-review under responsibility of the scientific committee of the 5th International Conference on Renewable Energy and Environment Engineering, REEE, 2022.

establishes the high-level DC voltage of the HVDC link directly, without high power step-up converter and offshore platform. In the series-connected topology, DC current of each DCWTs in the cluster is same. As the DC voltage of HVDC link is regulated to a constant value by receiving end converter, the output voltage of DCWTs will be unequal if wind speed is different. The output voltage of DCWT with lower wind speeds would be lower, making the rest of DCWTs undertake higher voltage and then be removed or limit the output power, resulting in energy curtailment [7,8]. In [9], an active overvoltage limitation strategy of the receiving end converter is proposed to protect the wind turbines from overvoltage damages, but fast communication is needed. An auxiliary voltage balance circuit is proposed to solve energy curtailment in [10]. In [11,12], a coordinate strategy is proposed for series-connected current source converter (CSCs), where DC current of the HVDC link is controlled by receiving end converter and energy curtailment is eliminated. In [13,14], CSC is substituted by FB-MMC as the minimum operation DC current limit of CSCs. However, the circulating current of offshore MMC converter should be carefully dealt and more devices are used with higher loss.

To overcome the problems existed, a novel coordinate control strategy is proposed for the series-connected DCWT based on SAB in this paper. The voltage balance mechanism of DCWF under unequal wind speeds is analyzed first. The characteristics of SAB are analyzed, and a coordinated control strategy for DCWF is proposed. The rest of this paper is organized as follows. Section 2 describes the DCWF configuration and steady-state operation principle. In Section 3, the coordinate control strategy with energy balancing and lower loss is presented. In Section 4, the simulation results of the validity for the proposed control strategy in PSCAD/EMTDC are presented. Section 5 is where the conclusions are found. The conclusions are obtained in Section 5.

## 2. Topology and operation principles

Fig. 1shows the configuration of the entire system, where an n×1 DCWF is integrated to the onshore grid. All DCWTs are series-connected to establish HVDC voltage. The FB-MMC-based converter is used as receiving end converter with its superior voltage control flexibility and fault blocking capability. The output power and voltage of the $i$th DCWT are $P_{(1,j)}$ and $V_{out(1,j)}$. The total DC voltage of the DCWF is $V_{WF}$, the DC voltage of receiving end is $V_{dc}$, and the DC current of HVDC link is $I_{dc}$. All DCWTs carry the same current, and the DC voltage of HVDC link $V_{WF}$ is the sum of the output voltage of DCWTs.

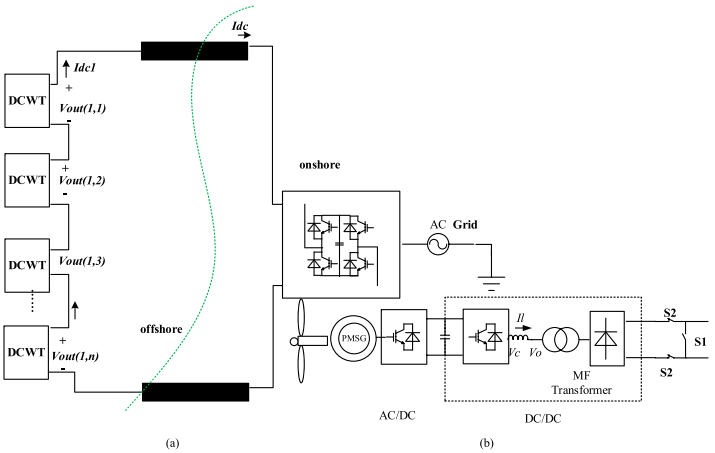


**Fig. 1.** (a) Topology of DC offshore wind farm, (b) Topology of DCWT.

The DCWT is composed by permanent magnet synchronous generator (PMSG), fully-rated AC/DC rectifier based on IGBT, and a DC/DC converter based on three-phase SAB to raise the lower DC voltage to higher DC voltage [3–5]. A medium frequency (MF) transformer, with lighter weight and smaller volume, is used in DC/DC converter for insulation. S1 is open during normal operation and is closed during startup and outage of the unit. S2 is closed and will be open during outage of the unit.

Usually, the receiving end converter operates in constant DC voltage control (CDV) mode or constant DC current (CDC) mode. The nominal output voltage $V_{out\_N}$ of DCWT and the average power $P_{avg}$ flow through the branch is

**Table 1**. Different output characteristics of CDV and CDC.

| | CDV | CDC |
|---|---|---|
| Limitations | $\begin{cases} V_{out\_N} = \dfrac{V_{dc}}{n} \\ P_{avg} = \dfrac{\sum_{j=1}^{n} P_{(1,j)}}{n} \end{cases}$ | $\begin{cases} V_{out\_N} = \dfrac{V_{dc}}{n} \\ I_{dc} = \text{const} \end{cases}$ |
| Output voltage | $V_{out(1,j)} = \frac{P_{(1,j)}}{P_{avg}} V_{out\_N}$ | $V_{out(1,j)} = \frac{P_{(1,j)}}{I_{dc}}$ |

shown in Table 1. It can be concluded that the wind speed variation would result in different DC voltage of DCWTs, and the output voltage of DCWTs with lower power output is lower, making other DCWTs tolerate higher DC voltage with the CDV mode. While in CDC mode, DCWTs with higher power output operate higher DC voltage and DCWTs with lower power output operate lower DC voltage, making the DCWTs operate independently and overvoltage of DCWTs is eliminated.

## 3. Control system

Traditionally, the AC/DC rectifier in DCWT controls active power to realize the maximum power point tracking (MPPT) of wind power and DC/DC converter controls the output DC voltage to maintain the energy balance of DCWT [7]. However, AC/DC rectifier will control the DC voltage at the desired value and keeps the energy balance of DCWT in this paper. As the DC voltage control by AC/DC has been well developed, only control strategy for DC/DC converter is presented in this chapter. So the novel control strategy for MPPT realized by DC/DC converter will be presented here.

### 3.1. DC/DC converter

The relationship of the output voltage of DC/DC $V_{out}$, AC voltage of medium frequency transformer $V_o$ and output DC current $I_{dc}$ is:

$$\begin{cases} V_{out} = aV_o - bI_{dc} \\ V_{out} = V_{dci} + I_{dc}R_{dc} \\ I_o = k_1 I_{dc} \end{cases} \tag{1}$$

where $a = 1.35N$, b $= 3\omega_F L_{TR}/\pi$, $k_1 = 0.78N$, $L_{TR}$, $\omega_F$ and $N$ are the equivalent reactance, operating frequency and ratio of MF transformer, $R_{dc}$ is the equivalent resistance of HVDC cable. According to (1), the conduction of the diode rectifier in DC/DC occurs only in the situation when $V_o$ is higher than its threshold value $V_{oth}$, which is determined by $V_{out}$ and referred as clamping characteristics.

Ignoring the loss of rectifier, the output power $P_{ac}$ can be gained as follows:

$$P_{ac} = P_{dc} = V_{out} I_{dc} = aV_o I_{dc} - b{I_{dc}}^2 \tag{2}$$

The relationship among $P_{ac}$, $V_o$ and $I_{dc}$ can be seen in (2). Assume that $I_{dc}$ is fixed, active power increases from 0 to the rated value when $V_o$ increase from $V_{oth}$ to 1pu.

Taking (2) into consideration, the active power delivered by DC/DC converter can be defined:

$$V_{oref} = K_{p\_P}(P_{ref} - P) + \frac{K_{i\_P}}{s}(P_{ref} - P) \tag{3}$$

where $P_{ref}$ and $P$ are reference values and output active power of DCWT and usually equals MPPT when wind speed is larger than the cut-in speed and lower than the rated speed. And a PI controller is used, where $K_{p\_P}$ and $K_{i\_P}$ are the proportion coefficient and integrator coefficient of the active power controller. The active power control makes that reference of $V_o$ increase or decreases to ensure the active power transmitted.

According to Fig. 1, dynamic equation converter at the primary side of MF in the DC/DC converter is expressed in $dq$ synchronous reference frame:

$$L_f \frac{d}{dt} I_{ldq} = \omega_F L_f I_{lqd} + V_{odq} - V_{cdq} \tag{4}$$

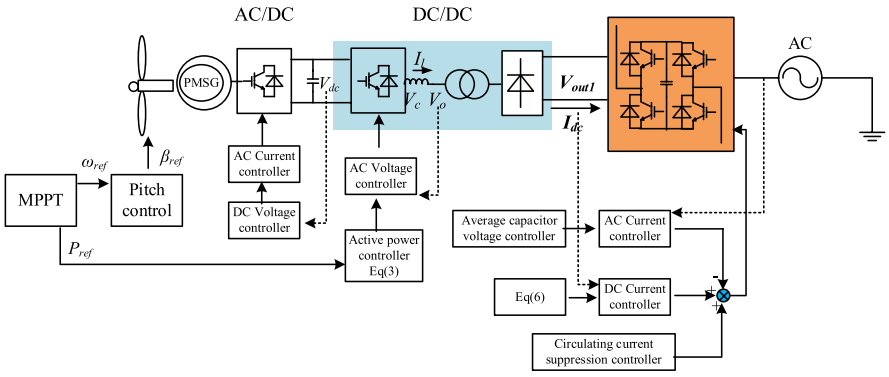


**Fig. 2.** Control block for the whole system.

where $L_f$ is the equivalent inductance, $I_{ldq}$ is the $d$-axis and q-axis components of current flow through inductance, $V_{cdq}$ is the d-axis and $q$-axis components of modulation voltage of inverter in DC/DC converter and $V_{odq}$ is the $d$-axis and $q$-axis components of AC voltage of MF. According to (4), a single-loop voltage control strategy can be used to control the AC voltage of MF transformer [15]. The control block for DC/DC is shown in Fig. 2. With the double loop voltage controller, AC voltage $V_o$ is controlled to its reference $V_{oref}$ and generates modulation voltage reference $V_{cdqref}$. With $V_o$ being controlled, the output voltage of DCWT can be controlled indirectly according to (1). $1.2V_{oref}$ is adopted as the upper limit $V_{max}$, and 0 is the lower limit $V_{min}$. As $I_o$ is fixed since $I_{dc}$ is under CDC mode, the current loop can be eliminated.

### 3.2. DC current control

The flexible voltage capability of FB-MMC makes it can be controlled as a current source. The controller of DC current for FB-MMC has been illustrated in [16,17] and will not be presented here. However, the power loss of DC cables is influenced by the current flow through the HVDC link and maintains almost unchanged with different transmitted power scenarios, making the transmission efficiency lower. The system safe operation limitation is analyzed as follows:

$$\begin{cases} V_{out(1,j)} \leq V_{out\,\max} \\ I_{dc\,\min} \leq I_{dc} \leq I_{dcN} \end{cases} \tag{5}$$

where $V_{\text{outmax}}$ is the maximum output voltage of DCWT, $I_{\text{dcmin}}$ is the minimum DC current of HVDC link and $I_{\text{dcN}}$ is the rated DC current of HVDC link.

According to (5), the output DC voltage of DCWT will increase with the wind power, so a DC current controller based on piecewise function is shown in (6):

$$I_{dcref} = K_{pDC}(\max(V_{out(1,j)}) - V_{outN}) \tag{6}$$

where $V_{\text{outN}}$ is the rated power of DCWT, $K_{p\_DC}$ is the proportion coefficient of DC current controller. By controlling the maximum output voltage of DCWT, the minimum DC current is obtained with a lower power loss of the HVDC link.

## 4. Simulation

A complete DCWF is built in PSCAD/EMTDC. The onshore MMC converter's rated DC current and DC voltage are 1.5 kA and 640 kV, respectively. The series connected DCWF consists of 100 DCWTs rated at 10 MW, producing a maximum power of 1000 MW. Five aggregate 200 MW DCWTs (a series connected DCWT cluster with 20 DCWTs) are built to represent whole DCWF to gain a faster simulation speed. The DC voltages of DCWT1, DCWT2, DCWT3, DCWT4, DCWT5 are $v_{out1}$, $v_{out2}$, $v_{out3}$, $v_{out4}$ and $v_{out5}$, rated at 128 kV, and corresponding output active power are $P_1$, $P_2$, $P_3$, $P_4$ and $P_5$. Mechanical parts and generate-side converters of DCWT are equivalent to a DC source at 6 kV. An average model based on FB-MMC is used in simulation and the HVDC transmission cable is modeled as an equivalent resistance. The parameters of whole system are listed in Table 2.

**Table 2**. Parameter of the system.

| Onshore MMC | | Wind turbine | | DC/DC | |
|---|---|---|---|---|---|
| Rated power | 1000 MW | Rated power | 200 MW | Input voltage of DC/DC converter | 6 kV |
| DC voltage | ±320 kV | Rated frequency | 12 Hz | Output voltage of DC/DC converter | 128 kV |
| DC current | 1.6 kA | Rated voltage of generator | 3.6 kV | Rated DC current of DC/DC converter | 1.6 kA |
| Onshore grid voltage | 400 kV | | | Isolation transformer of DCWT | 250 Hz, Y/Δ, 3.3/66, leakage inductance, 1% |

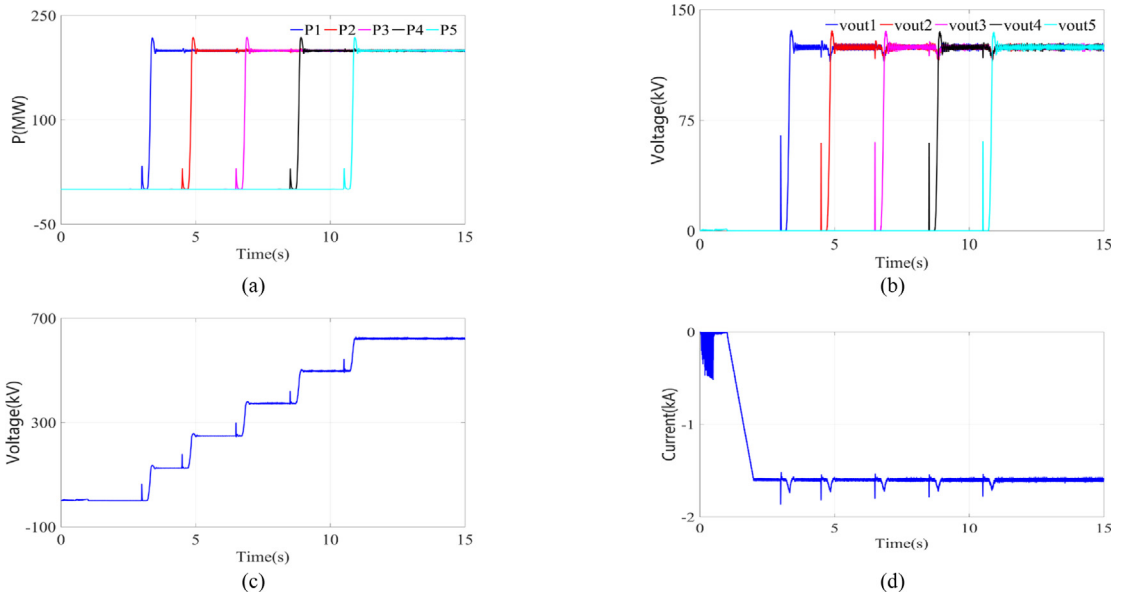


**Fig. 3.** Performance of DCWF during startup of, (a) Active power of DCWT, (b) Output voltage of DCWT, (c) DC voltage of DCWF, (d) DC current of HVDC link. (For interpretation of the references to color in this figure legend, the reader is referred to the web version of this article.)

### *4.1. Start-up*

The start-up of whole system is shown in Fig. 3. At $t = 0$ s, s1 of DCWT1 is opened and s2 is closed. Receiving end converter builds DC current through diode of DC/DC converter and reaches to 1.6 kA at $t = 2$ s as shown in Fig. 3(d) and DC voltage of receiving end converter is 0, as shown in Fig. 3(c).

At $t = 3$ s, DCWT1 start to generate power and its output power step from 0 to 200 MW, as the blue line in Fig. 3(a). With the increase of power, output voltage of DC/DC converter increase and reaches its rating voltage 122 kV, as the blue line in Fig. 3(b). Due to the small capacitor exist of DC/DC converter, a small overshoot is observed in Fig. 3(a) and (b). DC voltage of HVDC link reaches 122 kV in Fig. 3(c). At t = 4.5 s, DCWT2 is opened, start to generate power of 200 MW and DC voltage of HVDC link increase to 244 kV. As Fig. 3 shows, DCWTs are started one by one at t = 6.5 s, 8.5 s, 10.5 s. The DC current maintains at 1.6 kA during start up under the control of FB-MMC. The whole system starts up smoothly.

### *4.2. Output power under unequal wind speed*

The performance of DCWF under unequal wind speed is simulated. The output power of DCWT1, DCWT3, and DCWT4 are set to 200 MW, DCWT2 is set to 0 WM, and DCWT5 is set to 150 MW initially. The output voltage of DCWT1, DCWT3, and DCWT4 are 128 kV, DCWT2 is 0 kV, and DCWT5 is 95 kV correspondingly. The DC current is kept constant at 1.6 kA. There is no energy curtailment and overvoltage observed under unequal wind speed. At $t = 3$ s, the blue line in Fig. 4(a) shows that the power of DCWT1 drops to 0 MW while other DCWTs

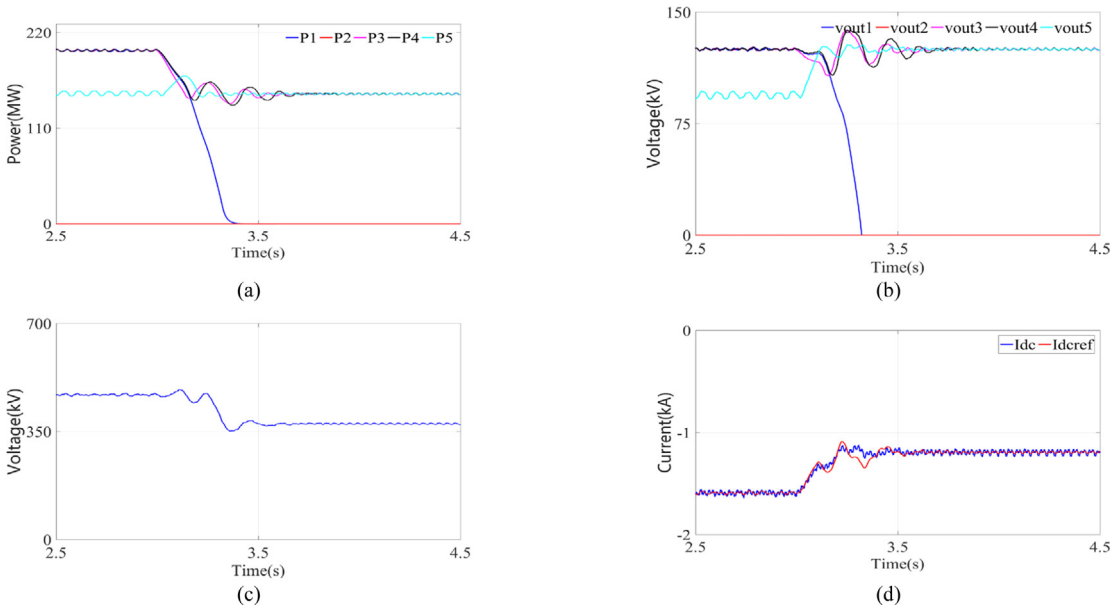


**Fig. 4.** Performance of DCWF during unequal wind speed (a) Active power of DCWT, (b) Output voltage of DCWT, (c) DC voltage of DCWF, (d) DC current of HVDC link. (For interpretation of the references to color in this figure legend, the reader is referred to the web version of this article.)

remain unchanged. In Fig. 4(b), the output voltage of DCWT5 increases to 125 kV with the control strategy of (6), the output voltage of DCWT1 decreases to 0 kV, and others remain unchanged. The DC voltage of the HVDC link decrease with the power, as shown in Fig. 4(c). The DC current is decreased to 1.1 kA with the power to reduce power loss of the HVDC link. It can be concluded that the system can operate safely with smaller power loss with the control strategy of (6).

## 5. Conclusion

A coordinate control strategy for series-connected DCWF is proposed in this paper, in which a receiving end converter based on FB-MMC acts as a DC current source and series-connected DCWTs based on SAB act as a DC voltage source with a larger DC voltage range. The linear relationship between active power, MF transformer AC voltage, output DC voltage, and output DC current of the SAB is investigated. It was discovered that adjusting the AC voltage of the MF transformer within a specified range can send active power to the DC grid. A power controller with double-loop for SAB is proposed, employing AC voltage of MF as an intermediate variable. The proposed coordinate strategy handles energy curtailment at unequal wind speeds without the use of an extra control method or equipment. A new DC current control approach for the receiving end converter is also presented to reduce the HVDC link's power loss. The proposed control strategy's effectiveness is confirmed by simulation results.

## Declaration of competing interest

The authors declare that they have no known competing financial interests or personal relationships that could have appeared to influence the work reported in this paper.

## Data availability

No data was used for the research described in the article.

## References

[1] Li Y, Guo J, Zhang X, Wang S, Ma S, Zhao B, Wu G, T. Wang over-voltage suppression methods for the MMC-VSC-HVDC wind farm integration system. IEEE Trans Circuits Syst II: Express Briefs 2020;67(2):355–9.

[2] Shi L, Adam GP, Li R, Xu L. Enhanced control of offshore wind farms connected to MTDC network using partially selective DC fault protection. IEEE J Emerg Sel Top Power Electron 2021;9(3):2926–35.
[3] Ma D, Chen W, Shu L, Qu X, Zhan X, Liu Z. A multiport power electronic transformer based on modular multilevel converter and mixed-frequency modulation. IEEE Trans Circuits Syst II: Express Briefs 2020;67(7):1284–8.
[4] Jing Y, Li R, Xu L, Wang Y. Enhanced AC voltage and frequency control of offshore MMC station for wind farm connection. IET Renew Power Gener 2018;12(15):1771–7.
[5] Hu P, Yin R, Wei B, Luo Y, Blaabjerg F. Modular isolated LLC DC/DC conversion system for offshore wind farm collection and integration. IEEE J Emerg Sel Top Power Electron 2021;9(6):6713–25.
[6] Pape M, Kazerani M. A generic power converter sizing framework for series-connected DC offshore wind farms. IEEE Trans Power Electron 2022;37(2):2307–20;
Veilleux E, Lehn PW. Interconnection of direct-drive wind turbines using a series-connected DC grid. IEEE Trans Sustain Energy 2014;5:139–47.
[7] Fu Y, Liu Y, Huang L-l, Ying F, Li F. Collection system topology for deep-sea offshore wind farms considering wind characteristics. IEEE Trans Energy Convers 2022;37(1):631–42.
[8] Zhang H, Gruson F, Rodriguez DMF, Saudemont C. Overvoltage limitation method of an offshore wind farm with DC series-parallel collection grid. IEEE Trans Sustain Energy 2019;10(1):204–13.
[9] Rong F, Wu G, Li X, Huang S, Zhou B. ALL-DC offshore wind farm with series-connected wind turbines to overcome unequal wind speeds. IEEE Trans Power Electron 2019;34(2):1370–81.
[10] Popat M, Wu B, Zargari NR. A novel decoupled interconnecting method for current-source converter-based offshore wind farms. IEEE Trans Power Electron 2012;27(10):4224–33.
[11] Popat M, Wu B, Liu F, Zargari N. Coordinated control of cascaded current-source converter based offshore wind farm. IEEE Trans Sustain Energy 2012;3(3):557–65.
[12] Wei Q, Wu B, Xu D, Zargari NR. A medium-frequency transformer-based wind energy conversion system used for current-source converter-based offshore wind farm. IEEE Trans Power Electron 2017;32(1):248–59.
[13] Guo G, Wang H, Song Q, Zhang Q, Rao H. Series-connected-based offshore wind farms with full-bridge modular multilevel converter as grid- and generator-side converters. IEEE Trans Ind Electron 2020;67(4):2798–809.
[14] Guo G, Wang H, Song Q, Zhang Q. HB and FB MMC based onshore converter in series-connected offshore wind farm. IEEE Trans Power Electron 2020;35(3):2646–58.
[15] Xie L, Yao L, Li Y, Xu L, Wang Z, Wei C, Cheng F. Frequency regulation participation of offshore wind farm integrated by diode-rectifer HVDC system. J Eng 2019;2019(16):977–81.
[16] Chen C, Adam GP, Finney S, Fletcher J, Williams B. H-bridge modular multi-level converter: control strategy for improved DC fault ride-through capability without converter blocking. IET Power Electron 2015;8(10):1996–2008.
[17] Adam GP, Davidson IE. Robust and generic control of full-bridge modular multilevel converter high-voltage DC transmission systems. IEEE Trans Power Deliv 2015;30(6):2468–76.